Nanowires for Integrated Multicolor Nanophotonics**

*Yu Huang, Xiangfeng Duan, and Charles M. Lieber**

***N**anoscale light-emitting diodes (nanoLEDs) with colors spanning from the ultraviolet to near-infrared region of the electromagnetic spectrum were prepared using a solution-based approach in which emissive electron-doped semiconductor nanowires were assembled with nonemissive hole-doped silicon nanowires in a crossed nanowire architecture. Single- and multicolor nanoLED devices and arrays were made with colors specified in a predictable way by the bandgaps of the III–V and II–VI nanowire building blocks. The approach was extended to combine nanoscale electronic and photonic devices into integrated structures, where a nanoscale transistor was used to switch the nanoLED on and off. In addition, this approach was generalized to hybrid devices consisting of nanowire emitters assembled on lithographically patterned planar silicon structures, which could provide a route for integrating photonic devices with conventional silicon microelectronics. Lastly, nanoLEDs were used to optically excite emissive molecules and nanoclusters, and hence could enable a range of integrated sensor/detection "chips" with multiplexed analysis capabilities.*

Keywords:
- electroluminescence
- LEDs
- nanowires
- optoelectronics
- photonics

Bottom-up assembly of nanoscale building blocks into increasingly complex structures offers the potential to produce devices with novel function since it is possible to combine in a general way materials with distinct chemical composition, structure, size, and morphology, in contrast to planar device fabrication.[1–3] Semiconductor nanowires (NWs)[1] and carbon nanotubes[3] are especially attractive building blocks for assembling active and integrated nanosystems since the individual nanostructures can function as both device elements and interconnects. This concept has been demonstrated in nanoelectronics with the assembly of a variety of devices, such as field-effect transistors (FETs)[4–7] and integrated NW logic gates,[8,9] and in nanophotonics with the assembly of, for example, individual light-emitting diodes[5,10] and laser diodes.[11]

The assembly of chemically distinct nanoscale building blocks that would otherwise be structurally and/or chemically incompatible in a sequential growth process typical of planar fabrication has received considerably less attention. However, this capability of the bottom-up approach should allow for assembly of nanostructures with function not readily obtained by other methods and open new opportunities. For example, planar silicon, which serves as the foundation for the microelectronics industry, is poorly suited to many photonic applications since it has a poor efficiency for light emission.[12] Here we demonstrate the assembly of a wide range of efficient direct-gap III–V and II–VI NWs with silicon NWs (SiNWs) and planar silicon structures to produce multicolor, electrically driven nanophotonic and integrated nanoelectronic–photonic systems. The flexibility of our approach suggests potential for applications in integrated sensor/detection systems, information storage, and other areas of photonics.

Our approach to nanoscale photonic devices is based upon sequential deposition of p-type and n-type NW materials into a crossed NW architecture using directed fluidic assembly[13] (Figure 1a), where the cross points are electri-

[*] Dr. Y. Huang, Dr. X. Duan, Prof. C. M. Lieber
Department of Chemistry and Chemical Biology, Division of Engineering and Applied Sciences
Harvard University
Cambridge, Massachusetts 02138 (USA)
E-mail: cml@cmliris.harvard.edu

[**] We acknowledge discussions with H. Park. This work was supported by the Air Force Office of Scientific Research and Defense Advanced Research Projects Agency. We thank Andrew Greytak for a gift of CdSe quantum dots.

Supporting information for this article is available on the WWW under http://www.small-journal.com or from the author.

DOI: 10.1002/smll.200400030

NANO MICRO small

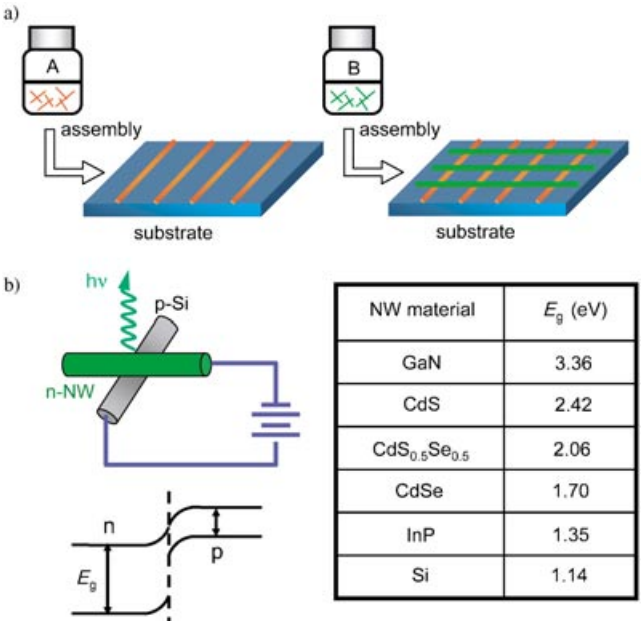

NW material	E_g (eV)
GaN	3.36
CdS	2.42
$CdS_{0.5}Se_{0.5}$	2.06
CdSe	1.70
InP	1.35
Si	1.14

Figure 1. a) Schematic of the assembly of crossed NW heterojunctions. First, a parallel array of A NWs (orange lines) is aligned on the substrate using a fluidic assembly method, and then a second parallel array of B NWs (green lines) is deposited orthogonally to achieve a crossed NW matrix; b) left: schematics showing a nanoLED structure formed between a p-SiNW and a direct bandgap n-type NW and its corresponding band diagram. Right: the table lists bandgaps of different materials (at 300 K) used in this study.

cally addressable. In the crossed NW p–n structure, the n-type NW is chosen to be a direct bandgap semiconductor with efficient light emission and the p-type material is silicon, which has an indirect bandgap and inefficient light emission (Figure 1b). The crossed NW heterostructures can be described qualitatively by a staggered type-II band diagram (Figure 1b, and Supporting Information),[14] and will emit light characteristic of the n-type NW element when the applied forward bias voltage exceeds the bandgap; the indirect-gap SiNW is a passive optical component and used for its well-defined electronic properties. Important features of the crossed NW nanoLED concept include: a) the emitted colors are limited only by the available direct-gap NW building blocks; b) the active device area is of nanometer dimensions, thus making these point light sources; c) the crossed NW architecture enables the formation of single- and multicolor arrays and integration of photonic and nanoelectronic elements, and d) the nanophotonic devices can be assembled on both rigid and flexible substrates.

The NW building blocks used in these studies, including direct bandgap III–V (e.g., GaN and InP) and II–VI (e.g., CdS and CdSe) materials, were prepared as single crystals by metal-nanocluster-catalyzed growth.[1,15] The bulk bandgaps of these semiconductors enable light emission from ultraviolet (UV, GaN) to near infrared (NIR, InP) as confirmed for individual NWs using photoluminescence measurements.[16,17] Electrical transport measurements made on individual NWs in a FET geometry showed that the GaN, CdS, CdSSe, CdSe, and InP NWs are all n-type with room-temperature electron mobilities (100–5000 $cm^2 V^{-1} s$)[7,18] that are comparable to bulk materials.[19] Previous studies have demonstrated that boron-doped p-type SiNWs exhibit carrier mobilities comparable to or better than bulk material.[6b,8]

Current–voltage (*I–V*) data for a typical p-Si/n-GaN crossed NW junction (Figure 2a) shows well-defined current rectification, as expected for a p–n diode with a turn-on voltage of approximately 1 V. These data are consistent with previous studies of n-GaN/p-Si diodes used as nanoelectronic logic gates.[8] The initial turn-on voltage, which approximates to the bandgap of Si, corresponds to injection of electrons into the SiNW from the n-GaN (see Supporting Information). Notably, applying a forward bias to the p–n junction of greater than bandgap of GaN yields strong electroluminescence (EL) at room temperature (Figure 2b). The EL spectrum shows a peak maximum at $\approx$365 nm consistent with the GaN band-edge emission, and demonstrates that crossed NW devices can function as UV nanoLEDs. Studies of over 30 n-GaN/p-Si nanoLEDs yielded similar *I–V* and EL results. Data plotted for four representative devices (Figure 2c) show several important points. First, light emission is detected when the bias voltage exceeds $\approx$3.5 V. This threshold is consistent with the 3.36 eV bandgap of GaN, which when exceeded, leads to radiative recombination of electron/hole pairs in GaN.[20] Second, the emission intensity increases rapidly with voltage and exhibits a nearly linear dependence on current above the threshold. The estimated quantum efficiency (electron to photon) is approximately 0.1%. This efficiency is less than commercial LEDs, although it could be improved by passivating surface traps and using a larger bandgap p-type NW for hole injection. Third, stable ($\geq$1 h) UV output is observed in air at room temperature at drive currents of $\approx$2 μA. Lastly, the near-field optical power densities, which are estimated 50 nm from a typical UV nanoLED, are on the order of 100 $W cm^{-2}$. Notably, this value exceeds that needed in a number of optical applications, such as lithography and spectroscopy.

Editorial Advisory Board Member

Charles M. Lieber is the Mark Hyman Professor of Chemistry and member of the Division of Engineering and Applied Sciences at Harvard University. He has pioneered the synthesis of a broad range of nanoscale materials, the characterization of the unique physical properties of these materials, and the development of methods of hierarchical assembly of nanoscale wires, together with the demonstration of applications of these materials in nanoelectronics, biological and chemical sensing, and nanophotonics. He is a member of the National Academy of Sciences, American Academy of Arts and Sciences, and fellow of the American Physical Society. He has published more than 230 peer-reviewed papers and is the principle inventor on more than 20 patents. He also founded the nanotechnology company, NanoSys, Inc.

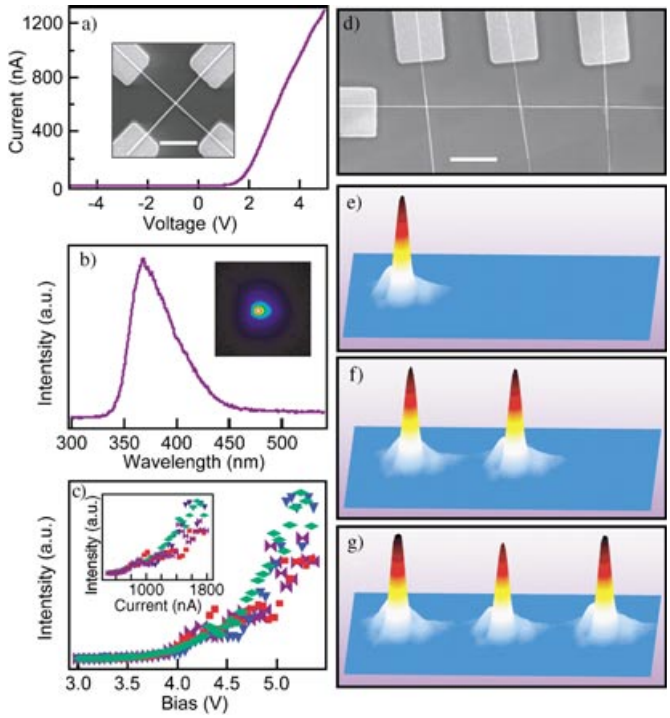

Figure 2. a) *I–V* data recorded for a p-Si/n-GaN crossed NW junction. Inset: scanning electron microscopy (SEM) image of a typical cross junction (scale bar = 1 μm); b) EL spectrum from the crossed p-Si/n-GaN NW nanoLED with a peak at ≈365 nm. Inset: EL image showing a spatial map of the intensity with a maximum at the NW cross point; c) emission intensity versus forward bias voltage for four distinct nanoLEDs. Inset: emission intensity versus injection current relationship for the same four nanoLEDs; d) representative SEM image of 3 p–n diodes formed by crossing three p-Si NWs over an n-GaN NW; scale bar is 2 μm; e–g) three-dimensional EL intensity plots of the three p–n diodes as a bias of 5.5 V is added sequentially to each Si NW with the GaN NW grounded.

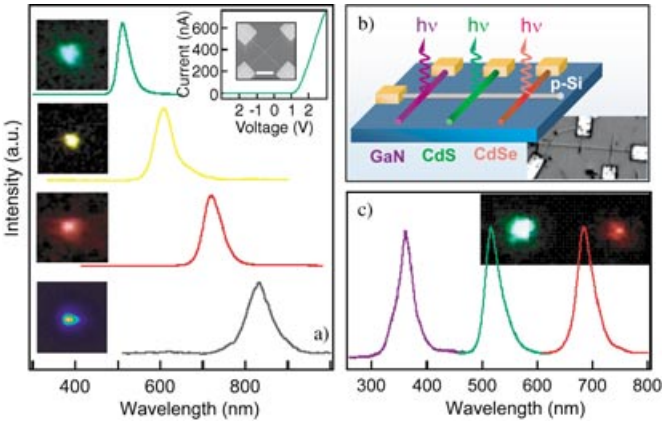

Figure 3. a) EL spectra from crossed p–n diodes of p-Si and n-CdS, CdSSe, CdSe, and InP, respectively (top to bottom). Insets to the left are the corresponding EL images for CdS, CdSSe, CdSe (all color CCD), and InP (liquid-nitrogen-cooled CCD) nanoLEDs. The inset top-right shows representative *I–V* and SEM data recorded for a p-Si/n-CdS crossed NW junction (scale bar = 1 μm); spectra and images were collected at +5 V); b) schematic and corresponding SEM image of a tricolor nanoLED array. The array was obtained by fluidic assembly and photolithography with ≈5 μm separation between NW emitters; c) normalized EL spectra and color images from the three elements.

The reproducibility and stability of the n-GaN/p-Si nanoLEDs suggests that they could be assembled into addressable arrays. To test this idea we used fluidic assembly[13] to make three junctions consisting of a n-GaN NW and three crossed p-Si NWs (Figure 2d). Transport measurements show that each of the three nanoscale junctions form independently addressable p–n diodes with clear current rectification. These p–n diodes each function as UV nanoLEDs, where each source can be individually switched on or off. Figure 2e–g shows a sequence of EL images where the three nanoLEDs were sequentially turned on, and demonstrate that the output intensity is similar for three sources. We believe these array results highlight the potential of the bottom-up approach for assembling integrated photonic devices, and should be important in exploiting such nanoLEDs in applications where parallel writing (e.g., lithography and information storage) and spectroscopy (e.g., integrated sensors) could be advantageous.

In addition, we assembled p–n junctions using p-Si NWs and a variety of other n-type NW materials, including CdS, CdSeS, CdSe, and InP to test whether our approach could yield nanoLEDs with a broad range of outputs. Transport measurements show that these p–n diodes behave similarly to p-Si/n-GaN p–n diodes. For example, *I–V* data recorded from a p-Si/n-CdS junction shows clear current rectification (inset, Figure 3a). When the CdS–Si NW diode forward bias voltage exceeds ≈2.6 V, strong light emission from the cross point is observed at room temperature. The emission maximum at ≈510 nm corresponds to CdS band-edge emission. Significantly, the light emission is so strong that it can be readily imaged with a color CCD camera and is visible to the naked eye in a dark room. The quantum efficiency of the CdS nanoLED device is estimated to be 0.1–1%, which is significantly higher than previously reported InP NIR (≈0.001%) and GaN (see above) nanoLEDs. The enhanced quantum efficiency may be explained in part by the intrinsically low surface state density for II–VI materials.[11,21] Moreover, studies of nanoLEDs based on CdSSe, CdSe, and InP NWs showed EL peak maxima and images characteristic of band-edge emission from the crossed junctions made with these materials: $CdS_{0.5}Se_{0.5}$, 600 nm; CdSe, 700 nm; and InP, 820 nm (Figure 3a).

We have exploited the ability to form nanoLEDs with nonemissive SiNW hole-injectors to assemble multicolor arrays consisting of n-type GaN, CdS, and CdSe NWs crossing a single p-type SiNW (Figure 3b). Normalized emission spectra recorded from the array demonstrates three spatially and spectrally distinct peaks with maxima at 365, 510, and 690 nm (Figure 3c) consistent with band-edge emission from GaN, CdS, and CdSe, respectively. In addition, color images of EL from the array shows the green and red emission from p-Si/n-CdS and p-Si/n-CdSe crosses, respectively (inset, Figure 3c). The ability to assemble different materials and independently tune the emission from each nanoLED offers substantial potential producing specific

NANO MICRO small

wavelength sources, and demonstrates an important step towards integrated nanoscale photonic circuits. Although lithography sets the integration scale of these multicolor arrays, it should be possible to create much denser nanoLED arrays via the controlled growth of modulated NW superlattice structures,[10] and/or the selective assembly of different semiconductor materials.[22]

In addition, we have assembled optoelectronic circuits consisting of integrated crossed NW LED and FET elements (Figure 4a). Specifically, in a two-by-one array, one GaN NW forms a p–n diode with the SiNW and a second GaN NW functions as a local gate as described previously.[8] Measurements of current and emission intensity versus gate voltage (Figure 4b) show that the current decreases rapidly with increasing voltage, as expected for a depletion mode FET, and that the intensity of emitted light also decreases with increasing gate voltage. When the gate voltage is increased from 0 to +3 V, the current is reduced from ≈2200 nA to an off state, where the supply voltage is −6 V. Advantages of this integrated approach include switching with much smaller changes in voltage (0–3 versus 0–6 V) and the potential for much more rapid switching. The ability to use the nanoscale FET to reversibly switch the nanoLED on and off is shown clearly in Figure 4c.

We have also investigated the potential of coupling the bottom-up assembly of nanophotonic devices described above together with top-down fabricated silicon structures, since this could provide a new approach for introducing efficient photonic capabilities into integrated silicon electronics. We implemented this hybrid top-down/bottom-up approach by using lithography to pattern p-type silicon wires on the surface of a silicon-on-insulator (SOI) substrate, and then assembling n-type emissive NWs on top of silicon structures to form arrays consisting of p–n junctions at cross points (Figure 5a). Conceptually, this hybrid structure (Figure 5b) is virtually the same as the crossed NW structures described above and should produce EL in forward bias. Notably, *I*–*V* data recorded for a hybrid p–n diode formed between the p-Si and an n-CdS NW show clear current rectification (Figure 5c) and sharp EL spectrum peaked at 510 nm (Figure 5d), which is consistent with CdS band-edge emission. To explore the reproducibility of this new hybrid approach we have also characterized arrays. For example, a 1×7 crossed array consisting of a single CdS NW over seven fabricated p-Si wires (Figure 5e) exhibits well-defined emission from each of the cross points in the array (Figure 5f). Similar results were obtained for two-dimensional arrays, and demonstrate clearly that bottom-up assembly has the potential to introduce photonic function into integrated silicon microelectronics.

The localized EL from crossed NW nanoLEDs and hybrid LEDs can result in near-field power densities greater than 100 W cm^{-2}, which is sufficient to excite molecular and nanoparticle chromophores. To explore this important possibility we use a CdS-based nanoLED to excite and record the emission spectra from CdSe quantum dots (QDs) and propidium iodide (a fluorescent nucleic acid stain; Figure 6). Notably, the emission of CdSe QDs and propidium iodide obtained by nanoLED excitation show essentially

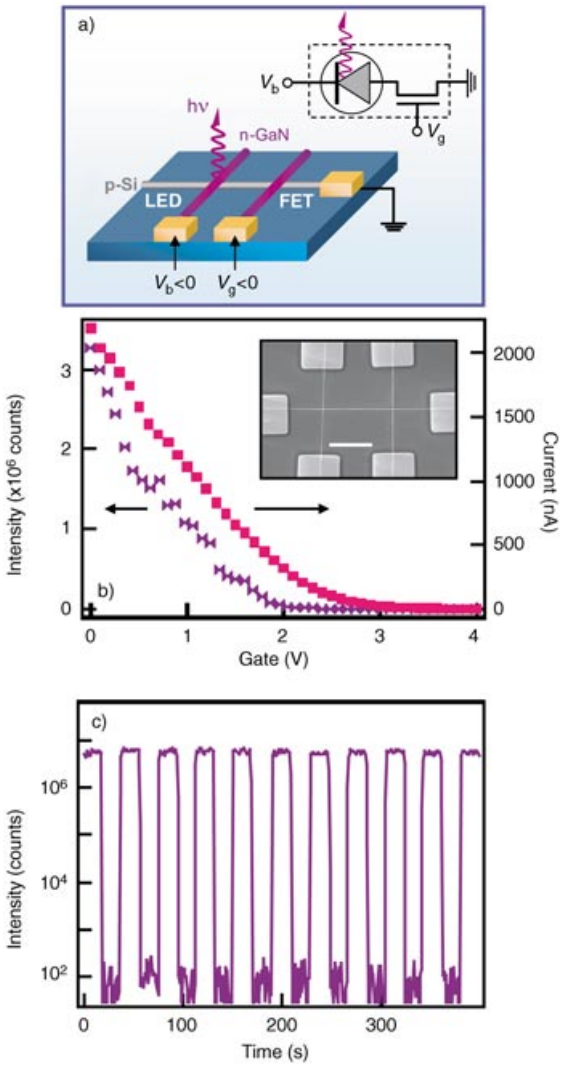

Figure 4. a) Schematic of an integrated crossed-NW FET and LED. The LED–FET array is obtained by crossing two n-GaN NWs with one p-Si NW. The p-Si NW is grounded and the first n-GaN NW is biased negatively, thus forming a forward-biased p–n diode that functions as an LED. The second n-GaN NW is positively biased, and forms a reverse-biased p–n diode with the grounded p-Si NW and blocks current through the second GaN NW. In this way, the positive-biased GaN NW can function as a local gate to modulate the current flow through the silicon NW and forms a nanoFET to modulate the current flow through the nanoLED and emission intensity of the nanoLED. Inset: a diagram of the equivalent circuit; b) plots of current and emission intensity of the nanoLED as a function of voltage applied to the NW gate at a fixed bias of −6 V. Inset: SEM image of a representative device (scale bar = 3 μm); c) EL intensity versus time relationship when a voltage applied to a NW gate is switched between 0 and +4 V for a fixed bias of −6 V.

the same spectra (solid lines, Figure 6a,b) as those obtained using much larger conventional excitation source (dashed lines, Figure 6a,b; see Experimental Section). These results demonstrate that nanoLEDs could function as excitation sources for integrated chemical and biological analysis.

In summary, we have demonstrated a broad range of multicolor and multifunction nanophotonic devices and small circuits assembled from semiconductor NW building

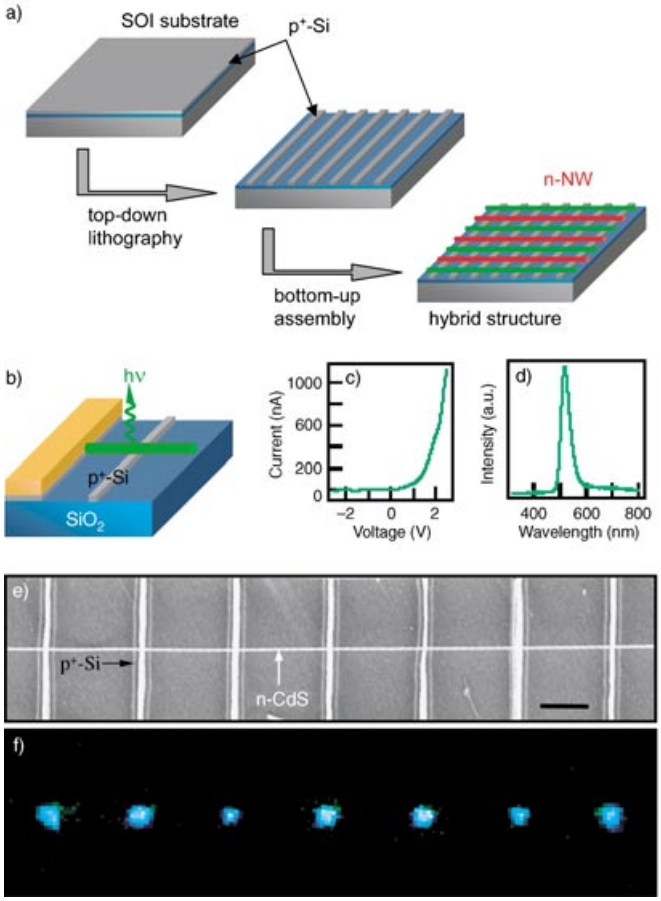

Figure 5. a) Schematic illustrating the fabrication of hybrid structures. A silicon-on-insulator (SOI) substrate is patterned by standard electron-beam or photolithography followed by reactive-ion etching. Emissive NWs are then aligned on to the patterned SOI substrate to form photonic sources; b) schematic of a single LED fabricated by the method outlined in (a); c) *I–V* behavior for a crossed p–n junction formed between a fabricated p^+-Si electrode and an n-CdS NW; d) EL spectrum from the forward-biased junction; e) SEM image of a CdS NW assembled over seven p^+-Si electrodes on a SOI wafer (scale bar = 3 μm); f) EL image recorded from an array consisting of a CdS NW crossing seven p^+-Si electrodes. The image was acquired with +5 V applied to each silicon electrodes while the CdS NW was grounded.

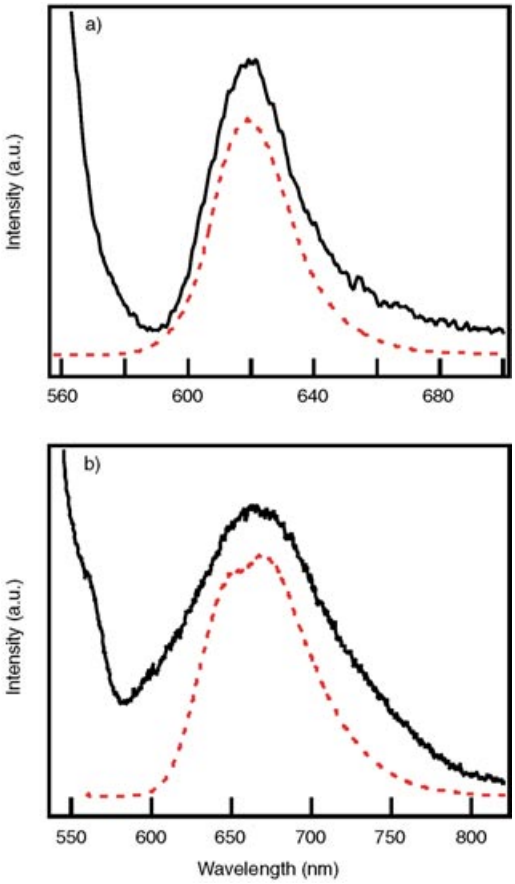

Figure 6. a) Emission spectrum (solid line) from CdSe QDs excited using a p-Si/n-CdS NW nanoLED; the QD emission maximum was 619 nm. The increasing intensity on the shorter wavelength side of the emission peak corresponds to the tail of the CdS nanoLED. The dashed red line is the spectrum of pure CdSe QDs excited with an Ar-ion laser; b) emission spectrum (solid line) from propidium iodide excited using a p-Si/n-CdS NW nanoLED. The dashed red line is the emission spectrum of propidium iodide obtained in aqueous solution (Fluorolog, ISA/Jobin Yvon-Spex).

blocks. We believe that these studies represent a new pathway towards integrated nanophotonic systems and could impact a number or areas including intra- and inter-chip optical interconnects and communications for the next generation of computing systems, ultrahigh density optical information storage, high-resolution microdisplays, and multiplexed chemical/biological analysis. Our studies demonstrate the potential of nanoLEDs in this latter area, and we believe this is especially promising since arrays of different color nanoLED sources could be combined with microfluidics in lab-on-a-chip systems to produce highly integrated analytic systems that might enable applications ranging from high-throughput screening to medical diagnostics.

Experimental Section

Nanowire synthesis: Compound semiconductor NWs (GaN, CdS, CdSSe, CdSe, InP) were synthesized using laser-assisted catalytic growth (LCG).[15a] The LCG target typically consisted of 95% of the respective semiconductor material and 5% Au as the catalyst. The furnace temperature was set at 700–900 °C during growth, and the target was placed at the upstream end of the furnace. A pulsed (8 ns, 10 Hz) Nd-YAG laser (1064 nm) was used to vaporize the target. Typically, growth was performed for 10 min with NWs collected at the downstream, cool end of the furnace. SiNWs were synthesized using a Au-nanocluster-catalyzed process using silane and diborane as reactant and dopant, respectively.[6a,15c]

Assembly of crossed NW devices: The crossed NW devices were assembled onto Si/SiO_2 substrates (600 nm oxide) using a layer-by-layer fluidic directed assembly.[13] Electrical contact patterns were defined using electron-beam lithography (JEOL 6400),

NANO MICRO small

and Ni/In/Au contact electrodes were thermally evaporated from pure metals. Electrical transport measurements of individual NWs or crossed NW junctions were made using a home-built system with <1 pA noise under computer control.

Optoelectrical characterization: Photoluminescence (PL) of individual NWs and electroluminescence (EL) of crossed NW junctions were characterized with a home-built microluminescence instrument.[5,17] PL or EL images were taken with a liquid-nitrogen-cooled CCD camera, and the spectra were obtained by dispersing emission with a 150 lines mm^{-1} grating in a 300 mm spectrometer.

Quantum dot and dye experiments: CdSe QDs were dispersed in hexane and then deposited over the nanoLED devices. An aqueous solution of propidium iodide (1 mg mL^{-1}; Molecular Probes, Inc.) was deposited directly onto a substrate containing p-Si/n-CdS NW nanoLEDs. Spectra were recorded from the NW cross points as described above and previously.[6,17] The emission spectrum of the propidium iodide aqueous solution was recorded using a commercial instrument (Fluorolog, ISA/Jobin Yvon-Spex).

[1] a) J. Hu, T. W. Odom, C. M. Lieber, *Acc. Chem. Res.* **1999**, *32*, 435; b) C. M. Lieber, *Sci. Am.* **2001** (September), 58; c) C. M. Lieber, *MRS Bull.* **2003** (July), 486; d) X. Duan, Y. Huang, Y. Cui, C. M. Lieber in *Molecular Nanoelectronics* (Eds.: M. A. Reed, T. Lee), American Scientific Publishers, New York, **2003**, pp. 199–227; e) Y. Cui, X. Duan, Y. Huang, C. M. Lieber in *Nanowires and Nanobelts—Materials, Properties and Devices* (Ed.: Z. L. Wang), Kluwer Academic/Plenum Publishers, Dordrecht, **2003**, pp. 3–68.

[2] a) A. P. Alivisatos, *Science* **1996**, *271*, 933; b) Z. L. Wang, *Adv. Mater.* **1998**, *10*, 13; c) M. Nirmal, L. Brus, *Acc. Chem. Res.* **1999**, *32*, 407; d) C. B. Murray, C. R. Kagan, M. G. Bawendi, *Annu. Rev. Mater. Sci.* **2000**, *30*, 545; e) W. J. Parak, D. Gerion, T. Pellegrino, D. Zanchet, C. Micheel, S. C. Williams, R. Boudreau, M. A. Le Gros, C. A. Larabell, A. P. Alivisatos, *Nanotechnology* **2003**, *14*, 15; f) M. A. El-Sayed, *Acc. Chem. Res.* **2004**, *37*, 326.

[3] a) Z. Yao, C. Dekker, P. Avouris, *Top. Appl. Phys.* **2001**, *80*, 147; b) P. L. McEuen, M. S. Fuhrer, H. Park, *IEEE Trans. Nanotechnol.* **2002**, *1*, 78; c) H. Dai, *Acc. Chem. Res.* **2002**, *35*, 1035.

[4] a) S. J. Tans, R. M. Verschueren, C. Dekker, *Nature* **1998**, *393*, 49; b) R. Martel, T. Schmidt, H. R. Shea, T. Hertel, P. Avouris, *Appl. Phys. Lett.* **1998**, *73*, 2447; c) V. Derycke, R. Martel, J. Appenzeller, P. Avouris, *Nano Lett.* **2001**, *1*, 453; d) A. Javey, J. Guo, Q. Wang, M. Lundstrom, H. Dai, *Nature* **2003**, *424*, 654.

[5] X. Duan, Y. Huang, Y. Cui, J. Wang, C. M. Lieber, *Nature* **2001**, *409*, 66.

[6] a) Y. Cui, C. M. Lieber, *Science* **2001**, *291*, 851; b) Y. Cui, Z. Zhong, D. Wang, W. U. Wang, C. M. Lieber, *Nano Lett.* **2003**, *3*, 149.

[7] Y. Huang, X. Duan, Y. Cui, C. M. Lieber, *Nano Lett.* **2002**, *2*, 101.

[8] Y. Huang, X. Duan, Y. Cui, L. Lauhon, K. Kim, C. M. Lieber, *Science* **2001**, *294*, 1313.

[9] A. Bachtold, P. Hadley, T. Nakanishi, C. Dekker, *Science* **2001**, *294*, 1317.

[10] M. Gudiksen, L. Lauhon, J. Wang, D. Smith, C. M. Lieber, *Nature* **2002**, *415*, 617.

[11] X. Duan, Y. Huang, R. Argarawal, C. M. Lieber, *Nature* **2003**, *421*, 241.

[12] P. Zhang, V. H. Crespi, E. Chang, S. G. Louie, M. L. Cohen, *Nature* **2001**, *409*, 69.

[13] Y. Huang, X. Duan, Q. Wei, C. M. Lieber, *Science* **2001**, *291*, 630.

[14] a) *Heterojunction Band Discontinuities* (Ed.: F. Capasso, G. Margaritondo), North-Holland, Amsterdam, **1987**; b) M. Leibovitch, L. Kronik, E. Fefer, V. Korobov, Y. Shapiraa, *Appl. Phys. Lett.* **1995**, *66*, 457.

[15] a) X. Duan, C. M. Lieber, *Adv. Mater.* **2000**, *12*, 298; b) X. Duan, C. M. Lieber, *J. Am. Chem. Soc.* **2000**, *122*, 188; c) Y. Cui, L. J. Lauhon, M. S. Gudiksen, J. Wang, C. M. Lieber, *Appl. Phys. Lett.* **2001**, *78*, 2214.

[16] Photoluminescence measurements were made on individual NWs using a home-built microluminescence instrument.[5,17] The data recorded on GaN, CdS, CdSeS, CdSe, and InP NWs typically showed luminescence maxima of $\approx$370, $\approx$510, $\approx$600, $\approx$700, and $\approx$820 nm, respectively, which are consistent with the bulk semiconductor bandgaps. The emission from InP NWs is blue-shifted due to quantum confinement and other factors.[5,17]

[17] M. S. Gudiksen, J. Wang, C. M. Lieber, *J. Phys. Chem. B* **2002**, *106*, 4036.

[18] Transport measurements were made on GaN, CdS, CdSeS, CdSe, and InP NWs in FET geometry with a back gate as described previously.[5-8] In all cases, positive gate voltage increases the conductance, and negative gate voltages decrease the conductance of the NWs, which is consistent with n-type doping. The carrier mobility of each material is estimated from the transconductance with values: GaN, 150–650 $cm^2V^{-1}s$; CdS, CdSSe, and CdSe, 100–400 $cm^2V^{-1}s$; and InP, 400–4000 $cm^2V^{-1}s$.

[19] O. Madelung in *LANDOLT-BORNSTEIN New Series: Vol III/22a, Semiconductors: Intrinsic properties of Group IV Elements and III–V and II–VI and I–VII Compounds* (Ed.: O. Madelung), Springer, Heidelberg, **1987**.

[20] Electrons are injected efficiently into the SiNW (from n-GaN NW) at the initial diode turn-on voltage of 1 V. Measurements in which the spectrometer detection range was extended to 1000 nm showed no evidence for bandgap emission from the SiNWs above the $\approx$1 V threshold.

[21] X. Duan, C. Niu, V. Sahi, J. Chen, W. Parce, S. Empedocles, J. Goldman, *Nature* **2003**, *425*, 274.

[22] S. R. Whaley, D. S. English, E. L. Hu, P. F. Barbara, A. M. Belcher, *Nature* **2000**, *405*, 665.

Published online on October 15, 2004

